Bioorganic & Medicinal Chemistry 18 (2010) 5602–5609

Contents lists available at ScienceDirect

Bioorganic & Medicinal Chemistry

journal homepage: www.elsevier.com/locate/bmc

Identification of a potent and noncytotoxic inhibitor of melanin production

Soonho Hwang [a], Sang Yoon Choi [b], Jin Hee Lee [c], Shinae Kim [a], Jinkyung In [a], Sang Keun Ha [b], Eunjung Lee [d], Tae-Yoon Kim [d], Sun Yeou Kim [b], Sun Choi [c], Sanghee Kim [a,*]

[a] College of Pharmacy, Seoul National University, San 56-1, Shilim, Kwanak, Seoul 151-742, Republic of Korea
[b] Graduate School of East-West Medical Science, Kyunghee University, 1 Hoegi, Dongdaemun, Seoul 130-701, Republic of Korea
[c] College of Pharmacy, Division of Life and Pharmaceutical Sciences, and National Core Research Center for Cell Signaling and Drug Discovery, Ewha Womans University, 11-1 Daehyun-Dong, Seodaemun, Seoul 120-750, Republic of Korea
[d] Laboratory of Dermatology-Immunology, College of Medicine, The Catholic University of Korea, 505 Banpo, Seocho, Seoul 137-040, Republic of Korea

ARTICLE INFO

Article history:
Received 8 May 2010
Revised 10 June 2010
Accepted 11 June 2010
Available online 17 June 2010

Keywords:
Biaryl amide library
Combinatorial chemistry
Depigmenting agents
Laplacian-modified naïve Bayesian
Structure–activity relationships

ABSTRACT

On the basis of a hit from random screening, biaryl amide derivatives were prepared in a combinatorial manner via parallel solution-phase synthesis, and their effects on melanocytes were investigated to discover new effective skin depigmenting agents. Among the 120 derivatives prepared, five members exhibited a >30% reduction of melanin production at 30 μM with a cell viability of >90%. In particular, compound **A_3/B_5** exhibited effective inhibitory activity on melanin synthesis. Although the inhibition percentage of **A_3/B_5** was slightly lower than that of the positive reference compound, phenylthiourea (PTU), **A_3/B_5** demonstrated a much better cell viability than PTU. In vivo evaluation of **A_3/B_5** also showed a significant decrease of melanin pigments. In addition, the in silico classification model was built based on the experimental data of library members. Our results suggest that these biaryl amide derivatives may act as potent skin depigmenting agents.

1. Introduction

The melanins are a group of complex phenolic biopolymers that are distributed widely in the natural world.[1] In animals, melanins are generated by melanocytes throughout the epidermis.[2,3] Melanins play a pivotal role in protecting the host from various types of ionizing sources such as free radicals and UV-radiation.[4] However, the increased production and accumulation of melanins induces a large number of hyperpigmentation diseases, including skin cancer, freckles, brown spots, and senescence spots.[5,6]

The melanogenesis pathway in mammals is controlled at many different levels.[1,7] A variety of proteins and enzymes, such as tyrosinase, tyrosinase-related protein-1 (TRP-1), and TRP-2, are known to be involved in the biosynthetic pathway. Several factors have been demonstrated to affect the activity of these enzymes and related proteins, and these factors include melanocyte stimulating hormone (MSH), basic fibroblast growth factor (bFGF), endothelin-1, and UV light.[8,9]

The key regulatory enzyme in the melanogenesis pathway is tyrosinase.[10] Thus, many efforts have been devoted to screening for inhibitors of this enzyme, and a majority of currently known depigmenting agents act directly or indirectly on this enzyme via several mechanisms.[11–13] Many chemical agents, including hydroquinone, arbutin, kojic acid, and phenylthiourea (Fig. 1), have been utilized for the treatment of hyperpigmentation disorders, but none are completely satisfactory owing to adverse effects such as toxicity.[11] Therefore, the development of ideal depigmenting agents is still in great demand. However, as far as we are aware,

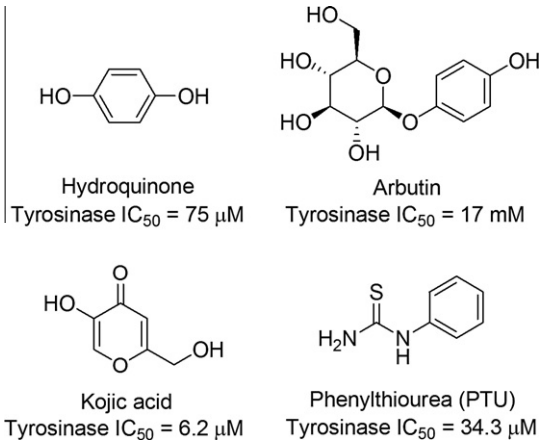

Figure 1. Structures and biological activity of representative depigmenting agents.

* Corresponding author. Tel.: +82 2 880 2487; fax: +82 2 888 0649.
E-mail address: pennkim@snu.ac.kr (S. Kim).

0968-0896/$ - see front matter © 2010 Elsevier Ltd. All rights reserved.
doi:10.1016/j.bmc.2010.06.034

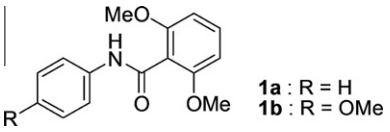

Figure 2. Chemical structure of compound **1**.

there has been little systematic medicinal chemistry research on the development of inhibitors of melanin production.

As a part of our efforts to discover new depigmenting agents, we have screened our compound collections. This resulted in the identification of compounds **1a** and **1b** (Fig. 2), which had modest potency with low cytotoxicity.[14,15] Unlike other most depigmenting agents, these compounds **1** had no effect on the tyrosinase enzyme function.[14,15] The biaryl amide template of **1** was attractive for a new class of depigmenting agents due to its simple structure, ease of synthesis, and chemical stability. As part of a continued effort to develop a potent melanin synthesis inhibitor, we report herein the generation of this class of compound library through an efficient solution-phase synthesis protocol, biological evaluations, and an in silico classification model based on the experimental data.

2. Results and discussion

2.1. Chemistry

The initial objective of our study was to identify analogues of compound **1** with improved potency without increased toxicity. To define the optimal substituents and their positions in the biaryl amide template, a series of biaryl amides was designed in a combinatorial manner and synthesized (Fig. 3 and Scheme 1). One factor to be considered in choosing the substituents on the aromatic rings was skin permeability. Since hydrophobic compounds tend to penetrate the skin much easier than hydrophilic compounds,[16] methyl and methoxy groups were primarily chosen as substituents in our studies.

We have previously reported a solution-phase strategy for the synthesis of a biaryl amide library that utilized Girard's reagent T as an acid chloride scavenger.[17] This clean, high-yielding protocol was employed in the present study. The selected 15 aryl amines **A** (**A_1**–**A_{15}**) (Fig. 3) were coupled with an excess (1.5 equiv) of eight different aromatic acid chlorides **B** (**B_1**–**B_8**) in the presence of Et_3N (2.0 equiv) and a catalytic amount of DMAP (0.1 equiv) in CH_2Cl_2 (Scheme 1). When total consumption of the amines was observed by thin layer chromatography, the reaction mixtures were purified by employing the work-up procedure previously described by us.[17] Briefly, the reaction mixture was treated with a solution of Girard's reagent T (**2**) in AcOH to convert the excess acid chlorides **B** to water soluble hydrazine derivatives **3**, and then the mixture was diluted with ethyl acetate. Subsequent washing with 1 N HCl, brine, saturated aqueous $NaHCO_3$, and brine, followed by concentration of the organic solution after drying over Na_2SO_4, yielded the desired combinatorial biaryl amide library consisting of 120 members **A_{1-15}/B_{1-8}**. In all cases, the members obtained after extractive work-up were virtually free from byproducts and impurities with an average HPLC purity of 98%.[18]

Figure 4 shows the distribution of the library members by the molecular properties: molecular weight, number of hydrogen-bond acceptors, *A*Log *P*, and polar surface area. The *A*Log *P* values

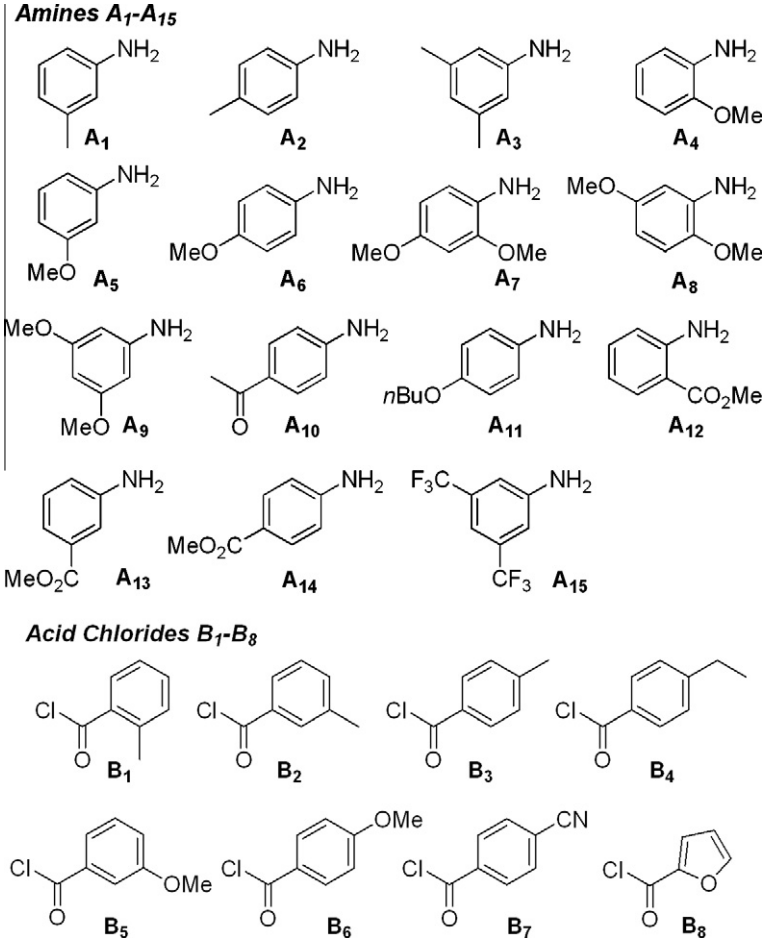

Figure 3. Building blocks, **A** and **B**, used for synthesis of the biaryl amide library.

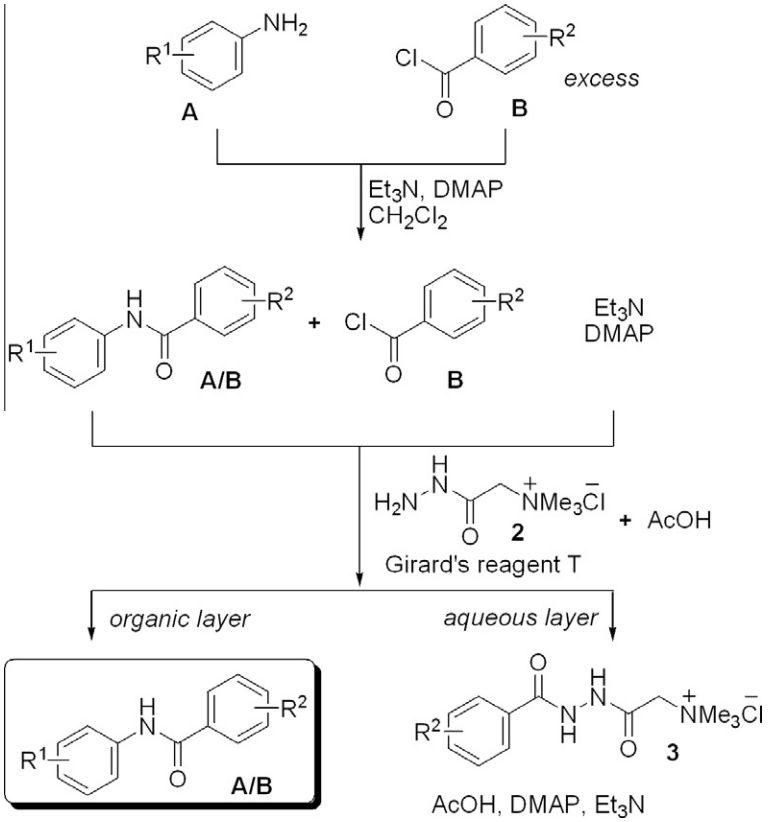

Scheme 1. Biaryl amide library synthetic route using Girard's reagent T.

of members were not extremely high. Although Lipinski's rule of five might not be accurately applied to the topical compounds, all of the members were drug-like according to the rule of five.

2.2. In vitro assays

To date, the in vitro screening of depigmenting agents depends predominantly on tyrosinase inhibitory activity.[19] However, many of the compounds having tyrosinase inhibitory activity failed to exert efficient inhibitory effects on melanin synthesis in melanocyte cells. For example, kojic acid, a well-known tyrosinase inhibitor, did not show significant depigmentation activity in either the melanocytes or in vivo.[20] Moreover, oxyresveratrol, which was identified as a potent tyrosinase inhibitor,[21] showed high cell toxicity in melanocyte cells.[14] Thus, we believed that the melanocyte assay was a more applicable and reliable method than the in vitro tyrosinase assay in terms of discovering compounds with both low toxicity and potent depigmentation ability.[14,15] In this study, we employed the melan-a melanocytes assay to identify effective depigmenting agents.

When screening combinatorial libraries, only one or two dilutions are generally tested, because multi-point assay for all samples is not common practice. Thus, we evaluated the biaryl amide library at a single concentration (30 μM). Although the tested concentration was somewhat high, we felt it was appropriate to identify the depigmenting compounds that have low cytotoxicity. The library members were dissolved in propylene glycol/EtOH/H_2O (5:3:2) solvent and added to the cell culture medium. There was no visible precipitation of library members from the complete assay solution.

The tests were conducted using cultured melan-a cells, and cell toxicity and melanin production were assessed. The results of the screening are summarized in Table 1. The known potent depigmenting agents phenylthiourea (PTU)[22,23] and compound **1b** were also tested for purposes of comparison. The level of reduced melanin was expressed as the difference between the percentage of cell viability and the percentage of melanin content to demonstrate the relative melanin content changes in only the viable cells. Among the members, $\mathbf{A_3/B_4}$ exhibited the highest reduction of melanin production (41.5%) with a cell viability of ca. 86%. The depigmenting activity and cell viability of compound $\mathbf{A_3/B_4}$ was higher than that of reference compound PTU at the tested concentration. A number of library members exerted a potent inhibitory effect on melanin production with a low cell toxicity; five members produced a >30% reduction in melanin production with a cell viability of >90%. For instance, $\mathbf{A_3/B_5}$ exerted no discernible cytotoxicity for cultured melan-a cells and showed considerably improved inhibitory effect on melanin production when compared with compound **1b**.

There appears to be a correlation between the cell viability and the substituent type at the biaryl amide template. For example, a majority of the library members of $\mathbf{A_{10}/B_x}$ and $\mathbf{A_{14}/B_x}$, having the electron withdrawing group at para position of aryl amines, showed a high level of cell viability. On the other hand, chemset $\mathbf{A_{15}/B_x}$, which contains the trifluoromethyl group, exhibited a profound reduction in cell viability. In addition, these data revealed that the locations of substituents on the template are also crucial in terms of affecting cell viability. For instance, chemsets $\mathbf{A_x/B_1}$, $\mathbf{A_x/B_2}$, and $\mathbf{A_x/B_3}$, which differed only in the positions of their methyl groups, showed differing levels of cell viability. The effects of library members on melanin production were also sensitive to the substitution pattern on the biaryl amide template. For example, chemsets $\mathbf{A_1/B_x}$, $\mathbf{A_2/B_x}$, $\mathbf{A_5/B_x}$, $\mathbf{A_6/B_x}$, $\mathbf{A_7/B_x}$, $\mathbf{A_8/B_x}$, $\mathbf{A_{10}/B_x}$, and $\mathbf{A_{11}/B_x}$ exerted no significant inhibitory effects on melanin production. However, chemsets $\mathbf{A_3/B_x}$, $\mathbf{A_{12}/B_x}$, $\mathbf{A_{15}/B_x}$, $\mathbf{A_x/B_3}$, $\mathbf{A_x/B_4}$, $\mathbf{A_x/B_5}$, $\mathbf{A_x/B_6}$, and $\mathbf{A_x/B_7}$ contained many members with notable depigmentation activity.

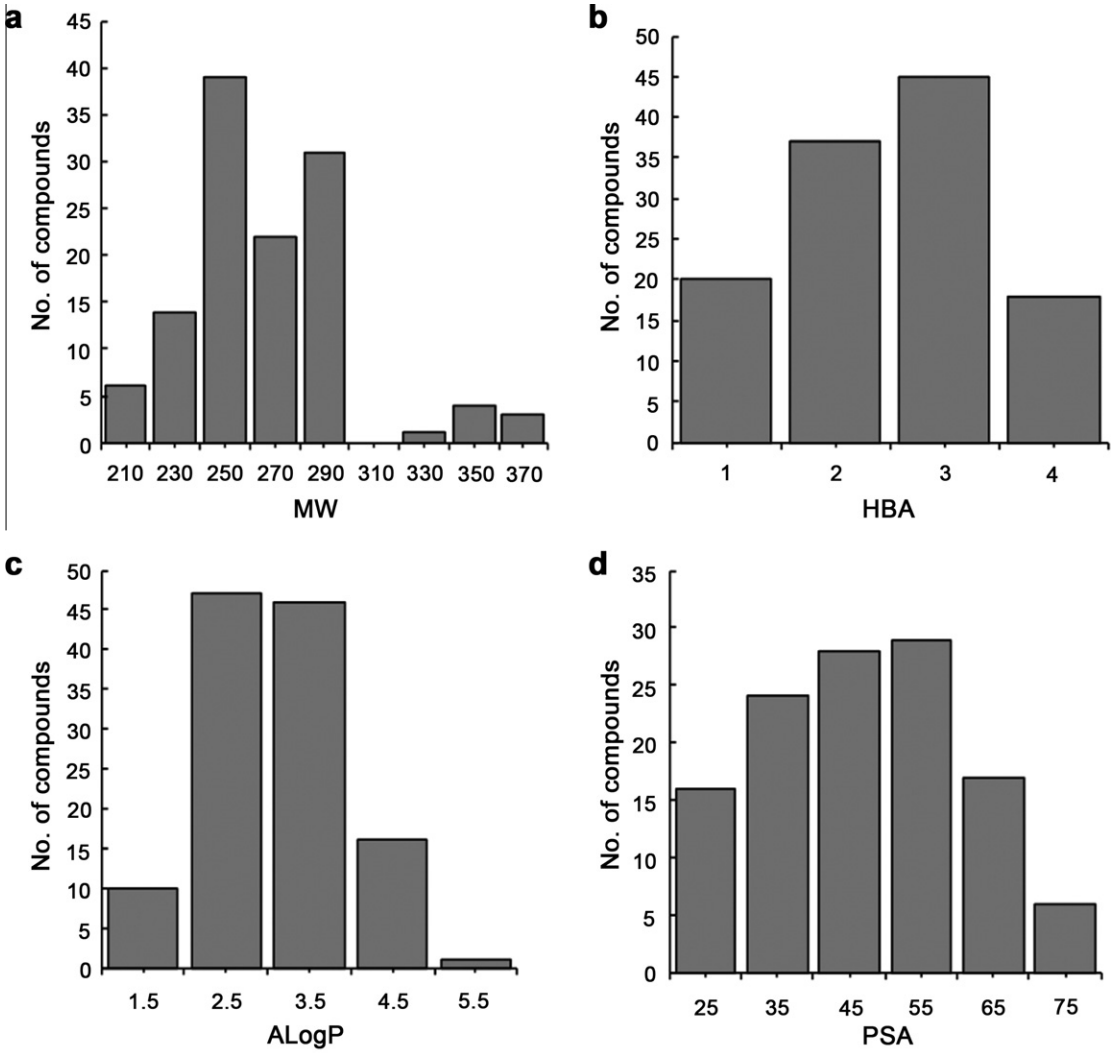

Figure 4. Distribution of the library members: (a) molecular weight (MW), (b) number of hydrogen-bond acceptors (HBA), (c) *A*Log *P*, (d) polar surface area (PSA).

2.3. Computational study

Since our preliminary results of quantitative structure–activity relationship (QSAR) and quantitative structure–property relationship (QSPR) analyses were not satisfactory, we decided to classify the depigmenting effect of biaryl amides. An in silico classification model was built by Laplacian-modified naïve Bayesian.[24,25] This is an effective machine learning method to classify actives from inactives, and has become more frequently used in recent drug discovery. One hundred and twenty compounds of the biaryl amide series with depigmenting activity values were used to build the classification model. If a library member had depigmenting activity greater than or equal to 20% with a cell viability of $\geqslant$80%, it was defined as active; other members were defined as inactive. All the data were split randomly into the training and test sets using the random percent filter of Pipeline Pilot,[26] resulting in 73 compounds in the training set and 47 compounds in the test set (as marked in Table 1). To obtain a reliable model, five descriptors were finally selected: *A*Log *P*, molecular weight, number of hydrogen-bond acceptors, polar surface area, and the extended-connectivity fingerprint (FCFP_8).[27] All of the compounds had one hydrogen-bond donor, so it was excluded from the descriptors.

In the model building, we used leave-on-out (LOO) cross-validation to avoid overfitting of the training set. Performance of the model was evaluated, and the accuracy, sensitivity, and specificity for the training set were 95.9%, 100%, and 95.5%, respectively. Those for the test set were slightly lower but satisfactory (details are as shown in Table 2.) The area under the receiver operating characteristic (ROC) score is a measure of the accuracy of a model, and this score between 0.9 and 1.0 is considered excellent.[28] In our model, the ROC scores were 0.96 and 0.90 in the training and test sets, respectively. An ROC plot is the true positive rate vs. the false positive rate, and the ROC plot of the test set was as shown in Figure 5a. An enrichment plot explains how fast all of the actives could be identified if the compounds were resorted by the model score.[29] Using the scores generated from our Laplacian-modified naïve Bayesian model, the enrichment plot revealed that 70% of the actives were found when ca. 10% of the compounds were tested (Fig. 5b). The overall results from our model showed that it was successful at classifying the data set compounds, and could be utilized to discover new biaryl amide templated depigmenting agents.

2.4. In vivo assays

Although a member $\mathbf{A_3/B_4}$ exhibited the highest inhibitory activity of melanin production, we were more interested in $\mathbf{A_3/B_5}$ because it manifested a profile superior to that of $\mathbf{A_3/B_4}$ in terms

Table 1
Biological data for compounds $\mathbf{A_{1-15}/B_{1-8}}$

A/B	Cell viability[a] (%)	Depigmenting effect[a,b] (%)	A/B	Cell viability (%)	Depigmenting effect (%)	A/B	Cell viability (%)	Depigmenting effect (%)
$\mathbf{A_1/B_1}$	87.5 ± 3.5	5.8	$\mathbf{A_6/B_1}$	97.8 ± 3.2	12.8	$\mathbf{A_{11}/B_1}$[d]	81.6 ± 4.0	9.9
$\mathbf{A_1/B_2}$	79.9 ± 3.9	−0.1	$\mathbf{A_6/B_2}$	94.0 ± 4.1	−0.4	$\mathbf{A_{11}/B_2}$	96.5 ± 1.4	4.8
$\mathbf{A_1/B_3}$[d]	96.1 ± 2.3	14.3	$\mathbf{A_6/B_3}$[d]	100.6 ± 1.8	4.9	$\mathbf{A_{11}/B_3}$	100.7 ± 1.5	−2.4
$\mathbf{A_1/B_4}$	100.0 ± 2.7	−2.2	$\mathbf{A_6/B_4}$[d]	76.5 ± 3.3	−9.9	$\mathbf{A_{11}/B_4}$	90.4 ± 2.6	−10.8
$\mathbf{A_1/B_5}$	103.1 ± 6.0	12.0	$\mathbf{A_6/B_5}$[d]	99.0 ± 4.1	0.5	$\mathbf{A_{11}/B_5}$[d]	90.4 ± 5.0	19.1
$\mathbf{A_1/B_6}$[d]	100.8 ± 4.2	−1.7	$\mathbf{A_6/B_6}$[d]	93.7 ± 2.8	−10.6	$\mathbf{A_{11}/B_6}$	97.1 ± 1.1	1.0
$\mathbf{A_1/B_7}$[d]	97.4 ± 5.2	11.1	$\mathbf{A_6/B_7}$[d]	98.5 ± 2.6	8.8	$\mathbf{A_{11}/B_7}$	89.0 ± 4.2	−4.4
$\mathbf{A_1/B_8}$	93.7 ± 1.9	−1.3	$\mathbf{A_6/B_8}$	95.5 ± 2.1	13.6	$\mathbf{A_{11}/B_8}$	87.8 ± 0.9	3.7
$\mathbf{A_2/B_1}$	85.4 ± 5.5	−0.2	$\mathbf{A_7/B_1}$[d]	95.5 ± 4.4	−3.5	$\mathbf{A_{12}/B_1}$	90.4 ± 6.5	9.7
$\mathbf{A_2/B_2}$[d]	67.4 ± 4.6	−2.4	$\mathbf{A_7/B_2}$[d]	103.2 ± 4.8	3.2	$\mathbf{A_{12}/B_2}$[d]	85.3 ± 3.9	29.6
$\mathbf{A_2/B_3}$[d]	86.0 ± 3.3	13.9	$\mathbf{A_7/B_3}$	99.4 ± 1.6	14.4	$\mathbf{A_{12}/B_3}$	90.1 ± 6.5	20.1
$\mathbf{A_2/B_4}$	75.1 ± 5.8	1.8	$\mathbf{A_7/B_4}$	78.5 ± 5.5	−6.5	$\mathbf{A_{12}/B_4}$[d]	91.9 ± 2.6	18.9
$\mathbf{A_2/B_5}$	84.6 ± 6.6	7.5	$\mathbf{A_7/B_5}$	98.9 ± 0.7	−3.9	$\mathbf{A_{12}/B_5}$	92.7 ± 5.3	11.1
$\mathbf{A_2/B_6}$[d]	99.8 ± 3.1	0.7	$\mathbf{A_7/B_6}$[d]	94.5 ± 3.2	−9.4	$\mathbf{A_{12}/B_6}$	98.2 ± 2.4	**31.1**[c]
$\mathbf{A_2/B_7}$	92.2 ± 5.3	10.9	$\mathbf{A_7/B_7}$	101.8 ± 3.3	7.2	$\mathbf{A_{12}/B_7}$[d]	99.6 ± 2.0	8.0
$\mathbf{A_2/B_8}$	100.2 ± 1.9	7.9	$\mathbf{A_7/B_8}$[d]	71.9 ± 5.9	−24.1	$\mathbf{A_{12}/B_8}$[d]	97.4 ± 4.3	−2.3
$\mathbf{A_3/B_1}$	101.7 ± 6.4	25.6	$\mathbf{A_8/B_1}$	95.6 ± 1.5	8.6	$\mathbf{A_{13}/B_1}$	99.2 ± 8.6	4.6
$\mathbf{A_3/B_2}$	81.0 ± 1.4	6.0	$\mathbf{A_8/B_2}$[d]	89.9 ± 5.3	0.3	$\mathbf{A_{13}/B_2}$	89.6 ± 2.2	10.5
$\mathbf{A_3/B_3}$	94.8 ± 4.8	**30.9**[c]	$\mathbf{A_8/B_3}$	84.1 ± 7.7	−3.2	$\mathbf{A_{13}/B_3}$	94.2 ± 0.9	16.4
$\mathbf{A_3/B_4}$[d]	85.8 ± 10.6	41.5	$\mathbf{A_8/B_4}$	72.7 ± 2.7	−19.8	$\mathbf{A_{13}/B_4}$	79.7 ± 6.5	37.0
$\mathbf{A_3/B_5}$	100.4 ± 4.1	**32.0**[c]	$\mathbf{A_8/B_5}$	101.6 ± 5.0	17.8	$\mathbf{A_{13}/B_5}$[d]	92.4 ± 8.9	20.1
$\mathbf{A_3/B_6}$	90.5 ± 3.3	**31.9**[c]	$\mathbf{A_8/B_6}$	94.4 ± 5.2	−8.3	$\mathbf{A_{13}/B_6}$[d]	99.2 ± 4.7	18.8
$\mathbf{A_3/B_7}$[d]	98.4 ± 1.8	**31.6**[c]	$\mathbf{A_8/B_7}$	96.0 ± 3.6	−1.7	$\mathbf{A_{13}/B_7}$	86.4 ± 3.6	0.8
$\mathbf{A_3/B_8}$[d]	99.2 ± 1.9	14.2	$\mathbf{A_8/B_8}$[d]	91.6 ± 4.6	−17.0	$\mathbf{A_{13}/B_8}$[d]	92.5 ± 2.9	0.4
$\mathbf{A_4/B_1}$	87.0 ± 2.9	7.0	$\mathbf{A_9/B_1}$[d]	89.1 ± 3.0	6.4	$\mathbf{A_{14}/B_1}$	98.6 ± 3.1	0.8
$\mathbf{A_4/B_2}$	71.1 ± 6.7	11.1	$\mathbf{A_9/B_2}$	89.3 ± 2.9	−12.6	$\mathbf{A_{14}/B_2}$	98.7 ± 3.5	12.9
$\mathbf{A_4/B_3}$[d]	91.0 ± 3.5	18.5	$\mathbf{A_9/B_3}$	92.1 ± 3.1	19.2	$\mathbf{A_{14}/B_3}$	97.1 ± 4.2	11.2
$\mathbf{A_4/B_4}$	83.5 ± 3.1	13.5	$\mathbf{A_9/B_4}$	94.8 ± 5.4	10.1	$\mathbf{A_{14}/B_4}$	96.7 ± 6.1	2.0
$\mathbf{A_4/B_5}$	95.7 ± 2.4	10.1	$\mathbf{A_9/B_5}$	95.2 ± 0.9	9.6	$\mathbf{A_{14}/B_5}$	102.9 ± 2.0	13.7
$\mathbf{A_4/B_6}$[d]	94.0 ± 2.6	−2.6	$\mathbf{A_9/B_6}$[d]	93.6 ± 3.7	13.6	$\mathbf{A_{14}/B_6}$	96.2 ± 0.6	−5.6
$\mathbf{A_4/B_7}$	94.5 ± 1.8	−3.1	$\mathbf{A_9/B_7}$	97.9 ± 4.4	9.6	$\mathbf{A_{14}/B_7}$	97.4 ± 2.9	14.2
$\mathbf{A_4/B_8}$[d]	85.7 ± 6.3	−5.4	$\mathbf{A_9/B_8}$[d]	93.7 ± 1.9	−1.3	$\mathbf{A_{14}/B_8}$[d]	85.6 ± 3.7	−8.4
$\mathbf{A_5/B_1}$[d]	93.4 ± 2.5	13.4	$\mathbf{A_{10}/B_1}$[d]	97.9 ± 1.8	0.1	$\mathbf{A_{15}/B_1}$	35.5 ± 6.0	15.1
$\mathbf{A_5/B_2}$	77.0 ± 6.9	−0.3	$\mathbf{A_{10}/B_2}$[d]	95.4 ± 3.8	−5.9	$\mathbf{A_{15}/B_2}$[d]	90.4 ± 4.2	−2.3
$\mathbf{A_5/B_3}$	100.0 ± 3.4	2.7	$\mathbf{A_{10}/B_3}$[d]	98.0 ± 0.5	11.2	$\mathbf{A_{15}/B_3}$	69.7 ± 2.2	0.3
$\mathbf{A_5/B_4}$	66.3 ± 7.4	6.3	$\mathbf{A_{10}/B_4}$[d]	99.7 ± 2.1	3.4	$\mathbf{A_{15}/B_4}$	30.5 ± 3.9	16.5
$\mathbf{A_5/B_5}$[d]	90.8 ± 3.0	−8.4	$\mathbf{A_{10}/B_5}$[d]	96.3 ± 5.0	−5.0	$\mathbf{A_{15}/B_5}$	45.5 ± 3.2	9.0
$\mathbf{A_5/B_6}$	92.6 ± 2.1	0.6	$\mathbf{A_{10}/B_6}$[d]	96.2 ± 2.8	0.7	$\mathbf{A_{15}/B_6}$	37.4 ± 6.8	21.0
$\mathbf{A_5/B_7}$[d]	97.8 ± 0.6	−9.4	$\mathbf{A_{10}/B_7}$[d]	96.9 ± 4.8	6.9	$\mathbf{A_{15}/B_7}$	67.5 ± 7.0	33.3
$\mathbf{A_5/B_8}$	97.9 ± 3.1	0.4	$\mathbf{A_{10}/B_8}$	93.2 ± 3.3	−2.6	$\mathbf{A_{15}/B_8}$	72.1 ± 14.6	31.9
Vehicle	99.8 ± 2.4	0.0	**1b**	99.8 ± 3.9	10.2	PTU	81.1 ± 6.6	38.0

[a] Cell viability and depigmenting effect was tested at 30 μM.
[b] Depigmenting effect was expressed as the difference between the percentage of cell viability and the melanin content {cell viability (%) − melanin content (%)}.
[c] Bold-face indicates biaryl amide members with >30% depigmenting activity and >90% cell viability.
[d] In the Laplacian-modified naïve Bayesian classification model, these compounds were used as the test set.

Table 2
Results of the Laplacian-modified naïve Bayesian model

Set	Actives		Inactives		Acc (%)	Sen (%)	Spe (%)	ROC
	TP	FN	FP	TN				
Training	6	0	3	64	95.9	100	95.5	0.96
Test	3	1	2	41	93.6	75.0	95.4	0.90

TP: true positive, FN: false negative, FP: false positive, TN: true negative, Acc: accuracy, Sen: sensitivity, Spe: specificity, ROC: the area under the receiver operating characteristic curve scores, Definitions of the Acc, Sen, and Spe are described in Section 4.

of cell viability at the tested concentration (30 μM), and also exhibited a comparable inhibitory effect on melanin production. To assess the effect of $\mathbf{A_3/B_5}$ on the inhibition of pigmentation in vivo, it was resynthesized and purified by chromatography. Compound $\mathbf{A_3/B_5}$ (10 μg, 0.1% in propylene glycol/EtOH/H_2O) were applied topically to the UVB-stimulated hyper-pigmented[30] dorsal skin of brown guinea pigs. As shown Figure 6, Fontana masson staining showed a significant decrease in the amount of melanin pigment in the $\mathbf{A_3/B_5}$-treated brown guinea pig skin (Fig. 6b) compared to the control (Fig. 6c). This result indicated that $\mathbf{A_3/B_5}$ treatment effectively inhibited UVB-induced pigmentation and suggests that biaryl amide derivatives could act as efficient therapeutic agents for hyperpigmentation in skin.

3. Conclusion

In conclusion, our study was conducted using melanocytes to discover a compound that fulfills the requisite criteria of reducing melanin production and cell toxicity. Based on the structure of the hit from the screening, we designed and synthesized a series of biaryl amides in a combinatorial manner. The use of parallel solution-phase synthesis techniques enabled the rapid preparation and identification of optimal substituents for each aryl moiety examined. The selected compound exhibited an effective inhibitory activity on melanin synthesis, with low cell toxicity in melan-a cells and a significant decrease of melanin pigment in the UVB-stimulated hyper-pigmented brown guinea pig skin. Our findings indicate that these biaryl amide derivatives may act as potent skin depigmenting agents. Additionally, our in silico model, generated by Laplacian-modified naïve Bayesian, showed an effective classification of the actives from the inactives and could be utilized for the prediction of new depigmenting agents. In addition, we believe

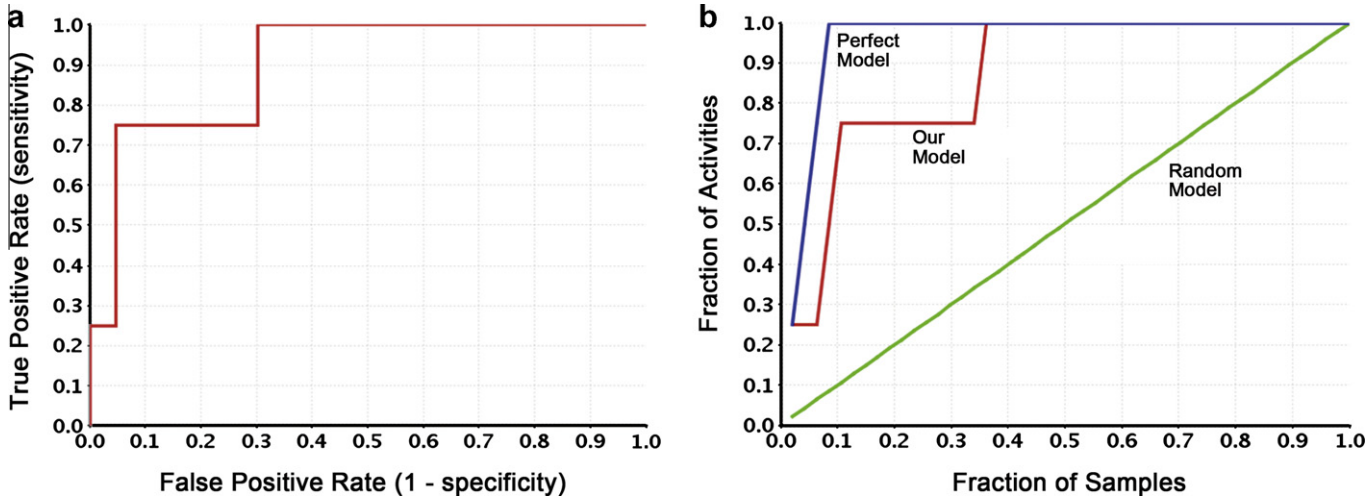

Figure 5. ROC and enrichment plots of the Laplacian-modified naïve Bayesian model for the test set. (a) ROC plot. (b) Enrichment plot of our model (red), compared with those of the perfect model (blue) and random model (green).

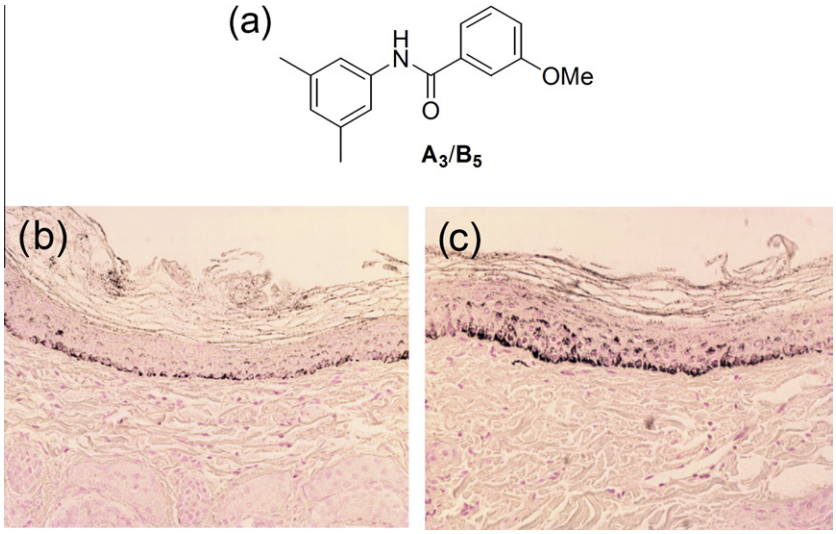

Figure 6. Chemical structure and effect of compound **A_3/B_5** on UV-induced pigmentation in brown guinea pig skin. (a) Chemical structure of **A_3/B_5**. (b) 10 μg of 0.1% **A_3/B_5** was applied topically twice a day for 4 weeks after the last UV tanning. (c) Control experiments were performed with use of the vehicle only.

that our study gives useful direction for further studies into the development of other suitable depigmenting agents. Detailed mechanistic studies directed towards identification of the molecular target of biaryl amides and biological evaluations of this newly disclosed class of depigmenting agents are ongoing and will be reported in due course.

4. Experimental

4.1. General

All chemicals were reagent grade and used as purchased. All reactions were performed under an inert atmosphere of dry argon or nitrogen using distilled dry solvents. Reactions were monitored by TLC analysis using Silica Gel 60 F-254 thin layer plates. ^{1}H NMR and ^{13}C NMR spectra were recorded in δ units relative to deuterated solvent as the internal reference at 300 or 400 MHz. Mass spectra (MS) were recorded using fast atom bombardment (FAB). High resolution mass spectra (HRMS) were recorded using FAB. Purities of products were determined by HPLC peak area analysis (ZORBAX Eclipse plus C18 column, 4.6 mm × 150 mm, 5 μm; ultraviolet absorption detector at 225 nm; gradient, 30–100% MeOH/H_2O, 40 min). Amines, aromatic acid chlorides, triethylamine, Girard's reagent T, and phorbol 12-myristate 13-acetate (TPA) were obtained from Sigma–Aldrich Inc. (USA). PTU was purchased from the TCI Co. (Japan). FBS, AA, and RPMI were purchased from Gibco BRL (USA). The melanin content and cell viability were measured using a Tecan Sunrise Remote microplate reader.

4.2. General procedure for parallel synthesis of biaryl amides

To a solution of aryl amine **A** (0.2 mmol) in CH_2Cl_2 (1 mL) was added acid chloride **B** (0.3 mmol), Et_3N (0.4 mmol), and a catalytic amount of DMAP (0.02 mmol). The mixture was stirred at room temperature for 5 h, after which a solution of Girard's reagent T in AcOH (0.5 M, 0.5 mL) was added. It was stirred overnight at room temperature and then diluted with ethyl acetate (3 mL). The reaction mixture was purified by subsequent washing with 1 N HCl (2 mL × 2), brine (2 mL), saturated aqueous $NaHCO_3$ (2 mL × 2), and brine (2 mL). The organic layer was passed through a short pad of drying agent (Na_2SO_4) and concentrated to give biaryl amide **A**/**B** (120 compounds). Purities of all products were

determined by HPLC peak area analysis. All operations in this synthesis were conducted on a Quest 210 parallel organic synthesizer, and solvent evaporation was performed on Genevac EZ-2 vacuum centrifuge.

4.3. Analytical data of representative biaryl amide compounds

Compounds **A_5/B_8**, **A_6/B_3**, and **A_6/B_5** were previously reported in 2002 by us.[17] However, HPLC purity, mass, and HRMS data were reanalyzed.

4.3.1. 4-Cyano-*N*-m-tolylbenzamide (A_1/B_7)

Yield 92%; ^{1}H NMR (400 MHz, CD_3OD) δ 8.05 (d, J = 8.4 Hz, 2H), 7.87 (d, J = 8.4 Hz, 2H), 7.51 (s, 1H), 7.47 (d, J = 8.2 Hz, 1H), 7.24 (t, J = 7.8 Hz, 1H), 6.99 (d, J = 7.0 Hz, 1H), 2.35 (s, 3H); MS (FAB): m/z (%): 237 (7) $[M+H]^+$, 176 (25), 154 (100), 136 (87); HRMS-FAB: m/z $[M+H]^+$ calcd for $C_{15}H_{13}N_2O$: 237.1028, found: 237.1033; purity by HPLC: 99.1%.

4.3.2. *N*-(3,5-Dimethylphenyl)-4-methylbenzamide (A_3/B_3)

Yield 91%; ^{1}H NMR (300 MHz, $CDCl_3$) δ 7.71 (d, J = 8.1 Hz, 3H), 7.24–7.22 (m, 3H), 6.75 (s, 1H), 2.38 (s, 3H), 2.28 (s, 6H); MS (FAB): m/z (%): 240 (72) $[M+H]^+$, 239 (51), 154 (100), 136 (72), 119 (47); HRMS-FAB: m/z $[M+H]^+$ calcd for $C_{16}H_{18}NO$: 240.1388, found 240.1379; purity by HPLC: 99.2%.

4.3.3. *N*-(3,5-Dimethylphenyl)-4-ethylbenzamide (A_3/B_4)

Yield 96%; ^{1}H NMR (300 MHz, $CDCl_3$) δ 7.74 (d, J = 8.3 Hz, 3H), 7.26–7.22 (m, 3H), 6.74 (s, 1H), 2.46 (q, J = 7.7 Hz, 2H), 2.27 (s, 6H), 1.22 (t, J = 7.7 Hz, 3H); MS (FAB): m/z (%): 254 (100) $[M+H]^+$, 133 (67); HRMS-FAB: m/z $[M+H]^+$ calcd for $C_{17}H_{20}NO$: 254.1545, found 254.1551; purity by HPLC: 99.6%.

4.3.4. *N*-(3,5-Dimethylphenyl)-3-methoxybenzamide (A_3/B_5)

Yield 94%; ^{1}H NMR (400 MHz, CD_3OD) δ 7.48–7.45 (m, 2H), 7.39 (t, J = 8.0 Hz, 1H), 7.29 (s, 2H), 7.11 (dd, J = 2.1, 8.2 Hz, 1H), 6.80 (s, 1H), 3.85 (s, 3H), 2.23 (s, 6H); MS (FAB): m/z (%): 256 (100) $[M+H]^+$, 255 (50), 154 (60), 135 (69); HRMS-FAB: m/z $[M+H]^+$ calcd for $C_{16}H_{18}NO_2$: 256.1338, found 256.1332; purity by HPLC: 99.4%.

4.3.5. 4-Cyano-*N*-(3,5-dimethylphenyl)benzamide (A_3/B_7)

Yield 95%; ^{1}H NMR (400 MHz, CD_3OD) δ 8.04 (d, J = 8.3 Hz, 2H), 7.87 (d, J = 8.4 Hz, 2H), 7.30 (s, 2H), 6.83 (s, 1H), 2.31 (s, 6H); MS (FAB): m/z (%): 251 (4) $[M+H]^+$, 176 (23), 154 (100), 136 (88); HRMS-FAB: m/z $[M+H]^+$ calcd for $C_{16}H_{15}N_2O$: 251.1184, found 251.1181; purity by HPLC: 99.4%.

4.3.6. *N*-(3-Methoxyphenyl)furan-2-carboxamide (A_5/B_8)

Yield 92%; ^{1}H NMR (300 MHz, $CDCl_3$) δ 8.17 (br s, 1H), 7.48 (dd, J = 0.9, 1.8 Hz, 1H), 7.45 (t, J = 2.1 Hz, 1H), 7.22 (m, 2H), 7.11 (ddd, J = 0.9, 1.8, 8.1 Hz, 1H), 6.69 (ddd, J = 0.9, 2.4, 8.4 Hz, 1H), 6.53 (dd, J = 1.8, 3.3 Hz, 1H), 3.80 (s, 3H); MS (FAB): m/z (%): 218 (47) $[M+H]^+$, 154 (100), 136 (74); HRMS-FAB: m/z $[M+H]^+$ calcd for $C_{12}H_{12}NO_3$: 218.0817, found 218.0814; purity by HPLC: 99.3%.

4.3.7. *N*-(4-Methoxyphenyl)-4-methylbenzamide (A_6/B_3)

Yield 93%; ^{1}H NMR (300 MHz, $CDCl_3$) δ 9.35 (br s, 1H), 7.88 (d, J = 8.4 Hz, 2H), 7.73 (d, J = 9.3 Hz, 2H), 7.28 (d, J = 8.4 Hz, 2H), 6.90 (d, J = 9.3 Hz, 2H), 3.77 (s, 3H), 2.38 (s, 3H); MS (FAB): m/z (%): 242 (19) $[M+H]^+$, 176 (25), 154 (100), 136 (77); HRMS-FAB: m/z $[M+H]^+$ calcd for $C_{15}H_{16}NO_2$: 242.1181, found 242.1174; purity by HPLC: 97.4%.

4.3.8. 3-Methoxy-*N*-(4-methoxyphenyl)benzamide (A_6/B_5)

Yield 92%; ^{1}H NMR (300 MHz, $CDCl_3$) δ 7.95 (br s, 1H), 7.53 (d, J = 9.0 Hz, 2H), 7.41 (m, 1H), 7.42–7.30 (m, 2H), 7.04 (ddd, J = 1.7, 2.6, 7.7 Hz, 1H), 6.87 (d, J = 9.0 Hz, 2H), 3.83 (s, 3H), 3.80 (s, 3H); MS (FAB): m/z (%): 258 (11) $[M+H]^+$, 176 (20), 154 (100), 136 (72); HRMS-FAB: m/z $[M+H]^+$ calcd for $C_{15}H_{16}NO_3$: 258.1130, found 258.1125; purity by HPLC: 97.3%.

4.3.9. *N*-(3,5-Dimethoxyphenyl)-4-methylbenzamide (A_9/B_3)

Yield 92%; ^{1}H NMR (300 MHz, CD_3OD) δ 7.80 (td, J = 2.0, 8.3 Hz, 2H), 7.30 (d, J = 7.9 Hz, 2H), 6.96 (d, J = 2.2 Hz, 2H), 6.27 (dd, J = 2.2, 2.4 Hz, 1H), 3.77 (s, 6H), 2.40 (s, 3H); MS (FAB): m/z (%): 272 (46) $[M+H]^+$, 154 (100), 136 (68), 119 (35); HRMS-FAB: m/z $[M+H]^+$ calcd for $C_{16}H_{18}NO_3$: 272.1287, found 272.1292; purity by HPLC: 99.5%.

4.3.10. Methyl 2-(4-methoxybenzamido)benzoate (A_{12}/B_6)

Yield 91%; ^{1}H NMR (400 MHz, CD_3OD) δ 8.75 (d, J = 8.5 Hz, 1H), 8.05 (dd, J = 1.2, 7.9 Hz, 1H), 7.94 (d, J = 8.8 Hz, 2H), 7.56 (dt, J = 1.4, 8.6 Hz, 1H), 7.11 (t, J = 7.4 Hz, 1H), 7.00 (d, J = 8.8 Hz, 2H), 3.94 (s, 3H), 3.85 (s, 3H); MS (FAB): m/z (%): 286 (9) $[M+H]^+$, 176 (18), 154 (100), 136 (75); HRMS-FAB: m/z $[M+H]^+$ calcd for $C_{16}H_{16}NO_4$: 286.1079, found 286.1081; purity by HPLC: 98.8%.

4.4. Biological assay

4.4.1. Cell line and culture procedure

A cell line of pigmented melanocytes, 'melan-a', was derived from normal epidermal melanoblasts from the embryos of inbred C57BL mice.[31] The melan-a cells were generously donated by Dr. B. G. Lee at the Skin Research Institute, Amore-Pacific Co, Korea. The cells were cultured at 37 °C under an atmosphere of 5% CO_2 in RPMI1640 medium with 10% FBS, 1% AA, and 200 nM phorbol 12-myristate 13-acetate (TPA). Melan-a cells were seeded at 105 cells/well in 24-well plates and incubated for 24 h. The media in each well were exchanged with 990 μL of medium each day and treated for three days with 10 μL of test samples. The test samples were dissolved in propylene glycol/EtOH/H_2O = 5:3:2 solvent.

4.4.2. Measurement of the cell viability

The percentage of viable cells was determined by staining the cells with crystal violet. After removing the medium from each well, the cells were washed with PBS. 200 μL of crystal violet (CV 0.1%, 10% EtOH, the rest was PBS) was added. The mixture was incubated for 5 min at room temperature and washed twice in water. After the addition of 1 mL of EtOH, the mixture was shaken for 10 min at room temperature. The UV absorption was measured at 590 nm.

4.4.3. Determination of the melanin level

After removing the media from each well, the samples were washed with PBS. This was followed by the addition of 1 mL of 1 N NaOH and shaking to dissolve the melanin. UV absorption was measured at 400 nm, and the percentage of melanin content per well was calculated by comparison with the controls.

4.4.4. UVB-induced hyperpigmentation in brown guinea pigs

UVB-induced hyperpigmentation was induced on the backs of the brownish guinea pigs weighing approximately 500 g using a slight modification of the methods reported by Ando et al.[32] and Imokawa et al.[33] The guinea pigs were anesthetized with pentobarbital (30 mg/kg), and separate areas (1 cm diametrical circle) of the back of each animal were exposed to the UVB radiation (Waldmann UV 800, Herbert Waldmann GmbH, Philips TL/12 lamp emitting 280–305 nm). The total UVB dose was 500 mJ/cm^2. Groups of four animals were used in the experiments. Animals were exposed to the UVB radiation once a week for three consecutive weeks. Ten micrograms of compound **A_3/B_5** (0.1% in propylene glycol/EtOH/H_2O = 5:3:2) was given topically to the hyper-pigmented areas

twice a day for 4 weeks from the next day of the last tanning. 4 weeks later, skin biopsies were carried out and processed for Fontana masson staining. Fontana masson staining was performed on 5 μm sections embedded in paraffin. The animals were housed and maintained in a barrier facility at the Institute for Animal Studies, School of Medicine, Catholic University of Korea. All of the animal protocols used in this study were approved by the Catholic Research Institute of the Medical Science Committee for Institutional Animal Care and Use.

4.5. Computational study

All computation calculations were undertaken on a Linux (Cent OS release 4.6) workstation.

4.5.1. Data set and descriptors

All of the compounds were sketched and cleaned up by Concord in Tripos SYBYL v.8.1.1. To generate the classification model, the data set was split into two groups, actives and inactives, and randomly divided into the training and test sets in a ratio of 1:1. The descriptors used in this study were: *A*Log *P*, molecular weight, number of hydrogen-bond acceptors, polar surface area, and the functional-class fingerprint (FCFP_8). FCFPs are 2D and extended-connectivity fingerprints based on the functional roles of an atom and its neighbors (i.e., hydrogen-bond donor/acceptor, positively/negatively ionizable, aromatic, and halogen). Splitting of data sets, calculation of descriptors, and building and evaluation of the classification model were carried out using SciTegic Pipeline Pilot v.7.5.2.

4.5.2. Laplacian-modified naïve Bayesian

The Bayesian classifier is a statistical modeling method based on Bayes's rule of conditional probability. The actual implementation of naïve Bayesian in Pipeline Pilot employs the Laplacian correction which assumes that the descriptors in the training set are independent and of equal importance.[24] This method produces a high-dimensional representation of the molecule by using extended-connectivity fingerprints. In this study, the model building and analysis were performed by Pipeline Pilot v.7.5.2 with the default parameters.

4.5.3. Model validation

The performance of classification model was evaluated by calculating the accuracy, sensitivity, and specificity, receiver operating characteristic (ROC) curve, and enrichment plot. Accuracy of a model is defined to correctly classify the actives from the inactives. Sensitivity is the ability of the model to avoid false negatives and specificity is its ability to avoid false positives. The accuracy, sensitivity, and specificity were calculated in the following way:

$$\text{Accuracy} = (TP + TN)/(TP + FN + TN + FP)$$
$$\text{Sensitivity} = TP/(TP + FN)$$
$$\text{Specificity} = TN/(TN + FP)$$

where TP is the number of true positives, TN is the number of true negatives, FP is the number of false positives, and FN is the number of false negatives.

Acknowledgments

This work was supported by the WCU program (R32-2008-000-10098-0) through KOSEF funded by MEST and the NCRC program (R15-2006-020) of the MEST and NRF through the Center for Cell Signaling & Drug Discovery Research at Ewha Womans University.

Supplementary data

Supplementary data associated with this article can be found, in the online version, at doi:10.1016/j.bmc.2010.06.034.

References and notes

1. Prota, G. *Pigment Cell Res.* **2000**, *13*, 283.
2. Sulaimon, S. S.; Kitchell, B. E. *Vet. Dermatol.* **2003**, *14*, 57.
3. Lin, J. Y.; Fisher, D. E. *Nature* **2007**, *445*, 843.
4. Sugumaran, M. *Pigment Cell Res.* **2002**, *15*, 2.
5. Urabe, K.; Nakayama, J.; Hori, Y. In *The Pigmentary System: Physiology and Pathophysiology*; Nordlund, J. J., Boissy, R. E., Hearing, V. J., King, R. A., Ortonne, J.-P., Eds.; Oxford University Press: New York, 1998; pp 909–911.
6. Cullen, M. K. In *The Pigmentary System: Physiology and Pathophysiology*; Nordlund, J. J., Boissy, R. E., Hearing, V. J., King, R. A., Ortonne, J.-P., Eds.; Oxford University Press: New York, 1998; pp 760–766.
7. Ito, S.; Wakamatsu, K.; Ozeki, H. *Pigment Cell Res.* **2000**, *13*, 103.
8. Martínez-Liarte, J. H.; Solano, F.; García-Borrón, J. C.; Jara, J. R.; Lozano, J. A. *J. Invest. Dermatol.* **1992**, *99*, 435.
9. Miyamura, Y.; Coelho, S. G.; Wolber, R.; Miller, S. A.; Wakamatsu, K.; Zmudzka, B. Z.; Ito, S.; Smuda, C.; Passeron, T.; Choi, W.; Batzer, J.; Yamaguchi, Y.; Beer, J. Z.; Hearing, V. J. *Pigment Cell Res.* **2007**, *20*, 2.
10. Wang, N.; Hebert, D. N. *Pigment Cell Res.* **2006**, *19*, 3.
11. Briganti, S.; Camera, E.; Picardo, M. *Pigment Cell Res.* **2003**, *16*, 101.
12. Okombi, S.; Rival, D.; Bonnet, S.; Mariotte, A.-M.; Perrier, E.; Boumendjel, A. *J. Med. Chem.* **2006**, *49*, 329.
13. Parvez, S.; Kang, M.; Chung, H.-S.; Cho, C.; Hong, M.-C.; Shin, M.-K.; Bae, H. *Phytother. Res.* **2006**, *20*, 921.
14. Choi, S. Y.; Kim, S.; Hwang, J. S.; Lee, B. G.; Kim, H.; Kim, S. Y. *Biochem. Pharmacol.* **2004**, *67*, 707.
15. Choi, S. Y.; Hwang, J. S.; Kim, S.; Kim, S. Y. *Biochem. Biophys. Res. Commun.* **2006**, *349*, 39.
16. Bos, J. D.; Meinardi, M. M. H. M. *Exp. Dermatol.* **2000**, *9*, 165.
17. Kim, S.; Ko, H.; Kim, S.; Lee, T. *J. Comb. Chem.* **2002**, *4*, 549.
18. See the Supplementary data for details.
19. Ando, H.; Kondoh, H.; Ichihashi, M.; Hearing, V. J. *J. Invest. Dermatol.* **2007**, *127*, 751.
20. Kong, Y. H.; Jo, Y. O.; Cho, C.-W.; Son, D.; Park, S.; Rho, J.; Choi, S. Y. *Biol. Pharm. Bull.* **2008**, *31*, 946.
21. Kim, Y. M.; Yun, J.; Lee, C.-K.; Lee, H.; Min, K. R.; Kim, Y. *J. Biol. Chem.* **2002**, *277*, 16340.
22. Poma, A.; Bianchini, S.; Miranda, M. *Mutat. Res.* **1999**, *446*, 143.
23. Kahn, V. *Pigment Cell Res.* **1995**, *8*, 234.
24. Xia, X.; Maliski, E. G.; Gallant, P.; Rogers, D. *J. Med. Chem.* **2004**, *47*, 4463.
25. The preliminary results of our quantitative structure–activity relationship (QSAR) and quantitative structure–property relationship (QSPR) analyses were not satisfactory.
26. Pipeline Pilot, http://accelrys.com.
27. Accelrys Software Inc., Chemistry Collection: Basic Chemistry User Guide, Pipeline Pilot Release 7.0, Accelrys Software Inc., San Diego, 2008.
28. Accelrys Software Inc., Data Modeling Collection: Basic Data Modeling User Guide, SciTegic Pipeline Pilot Release 7.0, Accelrys Software Inc., San Diego, 2008.
29. Sun, H. *ChemMedChem* **2006**, *1*, 315.
30. Bolognia, J.; Murray, M.; Pawelek, J. *J. Invest. Dermatol.* **1989**, *92*, 651.
31. Bennett, D. C.; Cooper, P. J.; Hart, I. R. *Int. J. Cancer* **1987**, *39*, 414.
32. Ando, H.; Ryu, A.; Hashimoto, A.; Oka, M.; Ichihashi, M. *Arch. Dermatol. Res.* **1998**, *290*, 375.
33. Imokawa, G.; Kawai, M.; Mishima, Y.; Motegi, I. *Arch. Dermatol. Res.* **1986**, *278*, 352.